# Preparation of thin film composite nano-filtration membranes for brackish water softening based on the reaction between functionalized UF membranes and…

Zarei, Farideh ; Moattari, M. Rozita ; Rajabzadeh, Saeid ; Bagheri, Maryam ; Taghizadeh, Abolfazl ; Mohammadi, Toraj ; Matsuyama, Hideto

(Citation)
Journal of Membrane Science,588:117207

(Issue Date)
2019-10-15

(Resource Type)
journal article

(Version)
Accepted Manuscript



(URL)
https://hdl.handle.net/20.500.14094/90008057

# Preparation of thin film composite nano-filtration membranes for brackish water softening based on the reaction between functionalized UF membranes and polyethyleneimine

Farideh Zarei[a1], Rozita M Moattari[a1], Saeid Rajabzadeh[*a,b], Maryam Bagheri[a], Abolfazl Taghizadeh[a], Toraj Mohammadi[**a], Hideto Matsuyama[b]

[1]*Center of Excellence for Membrane Science and Technology, Department of Chemical, Petroleum and Gas Engineering, Iran University of Science and Technology (IUST), Narmak, Tehran, Iran*

[b]*Research Center for Membrane and Film Technology, Department of Chemical Science and Engineering, Kobe University, Rokkodaicho 1-1, Nada, Kobe 657-8501, Japan*

*1 First and second author had equal contribution in this manuscript.*

*Corresponding author: E-mail: rajabzadehk@people.kobe-u.ac.jp

[b]Research Center for Membrane and Film Technology, Department of Chemical Science and Engineering, Kobe University, Rokkodaicho 1-1, Nada, Kobe 657-8501, Japan

**Corresponding author: E-mail: torajmohammadi@iust.ac.ir

Chemical, Petroleum and Gas Engineering School, Iran University of Science and Technology (IUST), Narmak, Tehran, Iran; Tel: +98 21 77240051; Fax: +98 21 77240051

## Abstract

A new method was developed to prepare a low-pressure nano-filtration membrane based on the membrane surface reaction (functionalized UF blend membrane) with polyethyleneimine (PEI) to fabricate thin film composite (TFC) membranes for water softening applications. The TFC selective layer was prepared by a reaction between the carboxyl functional groups of a carboxylated polyether sulfone (C-PES)/PES UF blend membrane and PEI. Hyper-branched PEI (HPEI) and PEI were used as poly-cations for fabricating the TFC NF membrane. Glutaraldehyde was used to cross-link the PEI on the membrane surface. The effects of the poly-cation concentration, crosslinker concentration, reaction time, reaction temperature, pH, and NaCl concentration as the supporting polyelectrolyte on the water permeability (WP) and rejection were evaluated. The addition of C-PES lead to the formation of finger-like structures and increased the water flux. While the effect of the polycation solution pH value was found to be the dominant parameter, optimization of the reaction time and concentration was necessary to obtain a membrane with acceptable water filtration capability. An NF membrane with WP as high as 10.1 LMH/bar and $MgCl_2$ (1000 ppm) rejection of 90% was obtained.

**Keywords**: Nano-filtration, Thin film composite membrane, Blend membrane, Membrane surface reaction, Surface functional groups, Crosslinking

## 1. Introduction

According to the World Resources Institute (WRI), significant threats to the potable water supply of the planet remain, particularly regarding the approximately one billion people living in water-scarce arid or semi-arid areas, and this number may increase to 3.5 billion by 2025 [1]. Moreover, technologies such as oil and gas, food, agricultural, textile, and dairy industries have further exacerbated the water shortage situation, indicating that the need for sources that produce fresh, clean water has become even more vital [2]. Accordingly, this problem has attracted the attention of many researchers around the globe to address water shortages by utilizing effective approaches such as desalination, purifying surface water, and effective treatment of wastewater.

Membrane-based water desalination techniques, especially reverse osmosis (RO), can be regarded as among the most promising methods to effectively reduce the global drinking water shortage [3, 4]. Furthermore, employing thin film composite (TFC) membranes with a polyamide rejection layer has proven to be the most critical and innovative aspect of an RO process [5]. However, RO technology suffers from severe challenges, such as high energy demand, high hydraulic pressure requirements, and intense membrane fouling [6]. Thus, despite many innovations in TFC membrane fabrication, the problem of energy consumption continues to be a major concern, and has encouraged researchers to seek new water desalination approaches [7].

In the late 1980's, the nano-filtration (NF) process was developed to fill the gap between ultrafiltration (UF) and RO processes in terms of operational considerations and energy consumption [8]. The NF process exhibits outstanding advantages compared to RO, such as low operating pressure, high water flux, highly efficient rejection of multivalent ions, the possibility of separating low molecular weight organic substances, as well as low operational and maintenance costs [9]. The most conventional applications of NF membranes are water softening, and removal

of heavy metals and organic compounds [10, 11]. Although in RO systems, TFC membranes with highly fine pore sizes are exploited, the NF process also employs similar TFC membranes with nominal pore sizes of less than 2 nm, which corresponds to a molecular weight cut-off (MWCO) range of 150–2000 Da [12]. This promising membrane system typically operates under a hydraulic pressure range of 5–10 bar. Interestingly, as the development of NF membranes with higher multivalent rejection matured, the required hydraulic pressure was found to decline continuously, which led to the establishment of the low-pressure NF process [13].

Despite its advantages, the NF process is a complex process which is not yet well understood. Further studies are needed for more effective realization of NF technology, especially regarding its separation efficiency [14]. The main separation mechanisms in the NF process are molecular sieving, cavity size, and ionic repulsion (surface charge) [9]. Membrane separation efficiency is strongly associated with surface properties and chemistry [15, 16].

The net surface charge of NF membranes can be negative, positive, or neutral [17]. Based on the Donnan electrostatic repulsion mechanism, a positively-charged NF membrane can effectively repel ions of similar charge. Thus, several attempts have been made to develop layers with positive surface charge along with increasing hydrophilicity to obtain higher water flux (WF), higher salt rejection, and lower membrane fouling to achieve high filtration NF membranes [18-20].

In this field of research, important findings have recently been reported. Wangxi Fang et al. utilized hyper-branched polyethyleneimine (HPEI) and TMC to fabricate a positively charged hollow fiber NF membrane via interfacial polymerization (IP) for low-pressure water softening in the presence of sodium dodecyl sulfate (SDS) in an HPEI solution [21]. They successfully fabricated a TFC membrane with a nominal pore size of approximately 1.29 nm, having a permeation of 17 LMH/bar, which was able to remove 96.7% and 80.6% of 1000 mg/L $MgCl_2$ and

$MgSO_4$, respectively, at 2 bar. Runnan Zhang et al. prepared a positively charged TFC NF membrane via IP of grafted fluorinated polyamine and PEI on a polydopamine (PDA) layer [22]. They enhanced the $MgCl_2$ and $CaCl_2$ rejections from 13.8% and 8.3% to 73.3% and 57.1%, respectively at a PDA deposition time, PEI concentration, and reaction temperature of 2 h, 2.0%, and 60 °C, respectively. In another study, Laurentia Setiawan et al. fabricated a positively charged dual-layer hollow fiber NF membrane from Torlon poly(amide-imide) (PAI) crosslinked on a PES substrate layer utilizing polyallylamine (PAAm) [23]. They achieved a saltwater permeability (SWP) of 15.8 LMH/bar as well as $MgCl_2$ and $CaCl_2$ rejections of 94.2% and 92.3%, respectively, under 2 bar hydraulic pressure. Later on, in an interesting study, Wangxi Fang et al., developed a reliable hollow fiber TFC-NF membrane with a nominal pore size of 1.27 nm via IP utilizing TMC, PEI, and piperazine on a PES substrate for low-pressure water softening [24]. They found that it is possible to improve the water permeability (WP) and $MgCl_2$ rejection up to 18.21 LMH/bar and 96.3%, respectively, by adding low amounts of PIP to the PEI solution. In further research, Rajabzadeh et al. developed an NF hollow fiber membrane by applying layer-by-layer PEI and poly (allylamine hydrochloride) (PAH) deposition on a porous substrate layer for low-pressure water softening [25]. They enhanced the SWP and $Mg^{2+}$ rejection to 12 LMH/bar and 94%, respectively, as they added low amounts of supporting electrolyte to the under-layers to optimize the pH. Subsequently, Chang Liu et al. developed a new approach to crosslink polyelectrolytes employing glutaraldehyde (GA) in LBL membrane fabrication [26]. They attained a pure WP of 10 LMH/bar and salt rejection higher than 95% for all $MgCl_2$, $MgSO_4$, and $Na_2SO_4$ salts under 2 bar of hydraulic pressure. The deposition of oppositely charged polyelectrolytes into a polyelectrolyte complex is another approach that has been used to fabricate a low-pressure NF hollow fiber membrane with a high permeation property. In this regard, Gherasim et al. [27]

deposited negatively charged poly(styrenesulfonate) and positively charged PEI/PDADMAC polyelectrolytes into a polyelectrolyte complex and then onto a PES-based polymer through a single-layer, dry-jet wet spinning process. The prepared hollow fiber membrane exhibited 7.6 LMH/bar permeability and ~90% rejection of $MgCl_2$, $MgSO_4$, and $Na_2SO_4$ at 2 bar pressure.

In a later attempt, Lim et al. [28] demonstrated that PAI/APTMS (aminopropyl tri-methoxy-silane) hollow fiber membranes had high hydrophilicity, exhibiting a permeability of 6.4 LMH/bar in isopropanol and 0.9 LMH/bar in dimethylformamide with Rose Bengal rejections of over 97% and 98%, respectively, under an operating pressure of 2 bar.

Integrating nanoparticles in the NF membrane structure can bring about some improvements. Li et al. [29] improved the permeate flux and antifouling characteristics of low-pressure NF membranes by embedding reduced graphene oxide-$NH_2$ (R-GO-$NH_2$) into the PA layer of NF composite hollow fiber membranes via IP. The fabricated membranes exhibited rejections of 26.9%, 98.5%, 98.1%, and 96.1% for NaCl, $Na_2SO_4$, $MgSO_4$, and $CaCl_2$, respectively. As another result of incorporating R-GO-$NH_2$, pure water flux increased from ~30.4 LMH to ~38.6 LMH at 2 bar.

In this study, a new functionalized UF blend membrane was prepared by blending C-PES with PES. Synthesized C-PES was developed using new materials, and a revised approach was used for obtaining completely reproducible results after we noted that the proposed methods were not easily reproducible. The prepared (C-PES)/PES blend membrane acted as a functionalized UF membrane active for PEI reaction to obtain a nanofiltration membrane. Adding a small amount of the synthesized C-PES (less than 1.5% in dope solution) drastically affected the membrane structure, water permeability (WP), and water contact angle of the prepared UF membrane. Within the scope of this study, a TFC NF membrane was developed using an entirely conventional, readily available,

low-cost material such as PES. As only a single layer of the reacted polycation was formed on the UF membrane and the dense layer thickness was very thin, high WP and acceptable divalent cation rejection were obtained. In contrast to the conventional interfacial polymerization (IP) method in which formation of pinholes and defects is a significant disadvantage, there were no observable defects or pinholes in the prepared membranes, which is an obvious advantage when applying the proposed membrane surface reaction method, rather than the conventional IP method. Despite the IP method being well developed, it generally (not always) results in low water permeability (<10 LMH/bar) and high salt rejection (>90% NaCl rejection). Therefore, achieving both high water permeability and high divalent and multivalent rejection is the main goal within the scope of the present study. However, the above-mentioned advantage of the developed method in the current study is only reliable at the lab-scale and its reliability at larger scales requires further research. The pH of the PEI solution had a very strong effect on the membrane filtration performance. The membrane WP and rejection results are explained based on the hypothesized C-PES and PEI reaction condition and polymer chemistry.

## 2. Materials and methods

### 2.1. Chemicals

Polyethersulfone (PES, MW= 58000, 6020) was obtained from BASF, Germany. Acetic anhydride, polyethylene glycol 200 (PEG-200), dimethylacetamide (DMAc), sodium chloride (NaCl), magnesium chloride ($MgCl_2$), and glutaraldehyde (GA, 25%) were purchased from Merck, Germany. Aluminum trichloride anhydrous ($AlCl_3$), potassium permanganate ($KMnO_4$), polyethyleneimine (PEI, MW=60 kDa), hyper-branched polyethyleneimine (HPEI, MW=750-

1000 kDa), and sodium hydroxide (NaOH) were procured from Sigma-Aldrich. N-Methyl-2-pyrrolidone (NMP, >99.5%) was obtained from Daejung, Korea.

### 2.2. Synthesis of carboxylated polyethersulfone (C-PES) and characterization

To obtain an NF membrane, a porous negatively charged support should be fabricated. In the current study, C-PES was selected as one of the starting materials for preparing a negatively charged UF support. The procedure by Wang et al., using the so-called controlled sequential acetylation and oxidation reactions, was followed to prepare C-PES [30]. In the course of the acetylation process, first, 10 gr of PES was added to and dissolved in 40 mL of NMP and was then heated to 90 °C in a three-neck round-bottom flask. Then, 41.6 mL of NMP as the solvent and 94.27 mL of acetic anhydride as the acetylation agent were added to 6.5 gr of $AlCl_3$ as the catalyst and stirred by a magnetic stirrer to obtain a completely uniform solution [31]. Later, the second solution was gradually added dropwise into the PES solution in the presence of nitrogen ($N_2$) gas to prevent side reactions, and the resulting solution was maintained under these conditions for 24 h to complete the reaction. After 24 h, the reaction solution was allowed to cool to room temperature. The complete reaction yielded a final solution with a light brown color. The acquired solution was then precipitated and rinsed with double distilled water until a neutral pH was achieved to ascertain the complete removal of any remaining acids. Afterward, the precipitated product was collected and dried in a vacuum oven at 60 °C for 24 h. For oxidation of the acetylated product, first, 10 gr of PES-$COCH_3$, which was synthesized in the acetylation stage, was dissolved into 40 mL of NMP at 80 °C. Later, 3.7 gr of NaOH as oxidation agent, 1.2 gr $KMnO_4$ as the catalyst, and 40 gr of NMP were added to 9 mL of double distilled water and then stirred until a uniform solution was obtained. The as-prepared solution was gradually added to the first solution and set aside for 6 h to allow the reaction to complete, finally resulting in a dark brown solution.

To separate the formed deposition, the solution was centrifuged at 4000 rpm for 40 min. Ultimately, the two-phase solution was placed in a vacuum oven and maintained for 12 h to acquire a red-color C-PES polymer [30, 31]. The overall carboxylation reaction of PES is illustrated in Fig. 1.

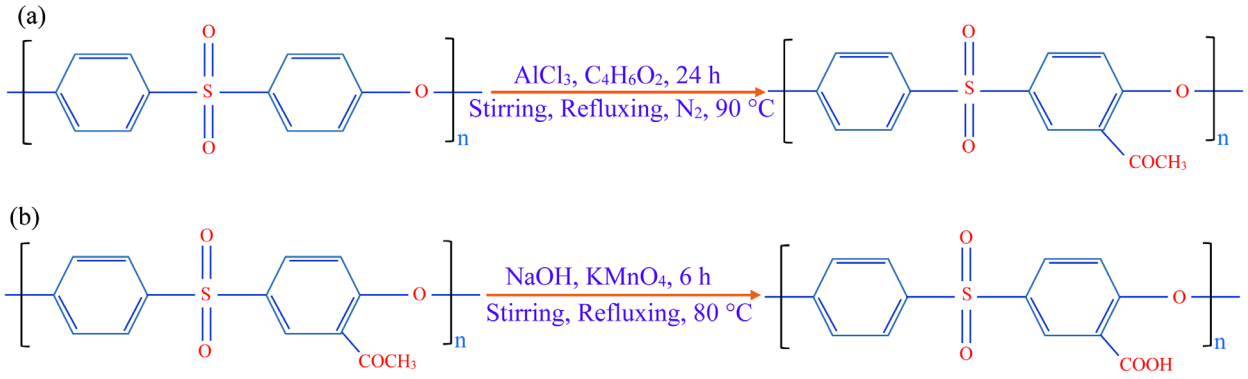


Fig. 1. Overall carboxylation reaction of PES to produce C-PES, a) acetylation, b) oxidation processes

Fourier transform infrared (FTIR, 8400 S) spectroscopy was employed to identify the chemical bonds of the PES, PES-$COCH_3$, and C-PES powders over the wavenumber range of 1500 $cm^{-1}$ to 4000 $cm^{-1}$. The hydrogen-1 nuclear magnetic resonance (H-NMR, 500 MHz) spectra of C-PES and PES-$COCH_3$ were also evaluated using an Avance III-500 MHz spectrometer (Bruker Co., Germany). Nota bene, all powder samples were dissolved in deuterated dimethyl sulfoxide solvent (DMSO-d6) before being evaluated by H-NMR.

### 2.3. Membrane preparation

Table 1 presents all the experimental conditions for the preparation of UF and NF membranes.

187 Table1. Membranes preparation conditions

| UF membranes | | | | | | | |
|---|---|---|---|---|---|---|---|
| **Membranes** | **(C-PES)/PES** | | **PES concentration (wt. %)** | | **PEG200 concentration (wt. %)** | | |
| M0 | 0/30 | | 18 | | 3 | | |
| M1 | 1/30 | | 18 | | 3 | | |
| M2 | 4/30 | | 18 | | 3 | | |
| **NF membranes** | | | | | | | |
| **Membranes** | **(C-PES)/PES** | **Temperature (˚C)** | **Reaction time (h)** | **pH** | **PEI concentration (wt. %)** | **GA concentration (wt. %)** | **Crosslinking time (min)** |
| M3 | 1/30 | 60 | 2 | 10.8 | 1.0 | 0.5 | 30 |
| M4 | 4/30 | 60 | 2 | 10.8 | 1.0 | 0.5 | 30 |
| M5 | 2/30 | 10-60 | 2 | 10.8 | 1.0 | 0.5 | 30 |
| M6 | 2/30 | 60 | 0.5-24 | 10.8 | 1.0 | 0.5 | 30 |
| M7 | 2/30 | 60 | 2 | 3-12 | 1.0 | 0.5 | 30 |
| M8 | 2/30 | 60 | 2 | - | 0.1-5 | 0.5 | 30 |
| M9 | 2/30 | 60 | 2 | 10.8 | 1.0 | 0.1-0.7 | 30 |
| M10 | 2/30 | 60 | 2 | 10.8 | 1.0 | 0.5 | 10-40 |

188

189 The conditions and the membrane preparation methods will be discussed in more details in the
190 following sections.

191 **2.3.1. Preparation of (C-PES)/PES asymmetric UF membrane**

192 (C-PES)/PES blend flat sheet asymmetric porous UF membranes were fabricated via the
193 conventional non-solvent-induced phase inversion method [32, 33]. The PES granules were placed
194 in an oven for 24 h at 110 °C to remove their moisture prior to blending with the synthesized C-
195 PES. First, 3.0% PEG-200 was dissolved into NMP, and then certain amounts of C-PES and PES
196 polymers were gradually added to the prepared mixture to obtain a dope with 18.0 wt. % total

polymer concentration with C-PES/PES ratios presented in Table 1.

The solution was then stirred at 250 rpm for 24 h followed by degassing at 65 °C for another 24 h in an oven. The prepared dope solution was cast on the typical non-woven supports and smoothed on a glass plate using a casting knife with gate adjustment of 150 μm, and then the cast film was immediately immersed in deionized (DI) water before characterization and before applying the thin film rejection layer.

### 2.3.2. Preparation of the surface active layer

A novel method, called the membrane surface reaction method, was employed to create the dense layer. In this method, the reaction between functional groups of UF membrane and a poly-cation agent occurs to prepare the surface active layer on the top surface of the prepared porous support. This method involves the reaction of a hyper-branched polycation with the surface of the UF membrane layer mainly induced by C-PES. In this approach, the（C-PES）/PES support layer, which is expected to be negatively charged at the top surface owing to the segregation of the C-PES (that will be discussed later) produces the reaction with hyper-branched PEI followed by crosslinking with PEI by adding given amounts of the GA monomer dissolved in water. It is noteworthy to state that PEI was employed as the polycation owing to its high molecular weight, water solubility, positive charge, and large amounts of branches to obtain the appropriate rejection layer as well as to provide more reaction bonds. The probable reaction between C-PES and PEI is illustrated in Fig. 2. First, PEI is dissolved in water according to Fig. 2(a), followed by reactions with C-PES functional groups (Fig. 2(b)). Later, a certain amount of PEI dissolved in water at a specified temperature was deposited on the top surface of the porous UF membrane layer and maintained to allow the reaction to complete within a given timeframe. Then, the reacted surface

was washed using sufficient DI water to remove any unreacted PEI molecules. The membrane surface reaction in this study was found to be a reversible endothermic reaction in which the forward reaction proceeds slowly. Although the reaction between PES-COOH and PEI was not studied, and further detail and accurate study are needed (we will address this gap in a separate paper), it has been reported that the carboxyl reaction with PEI is an endothermic and reversible reaction [34]. In other words, because the $H_2O$ molecule is a weak nucleophile, it has a low tendency to capture H ions from the amine functional group of PEI, leading to the deceleration of the forward reaction, which in turn provides reversibility of the reaction owing to the instability of the $H_3O^+$ present in the reaction medium.

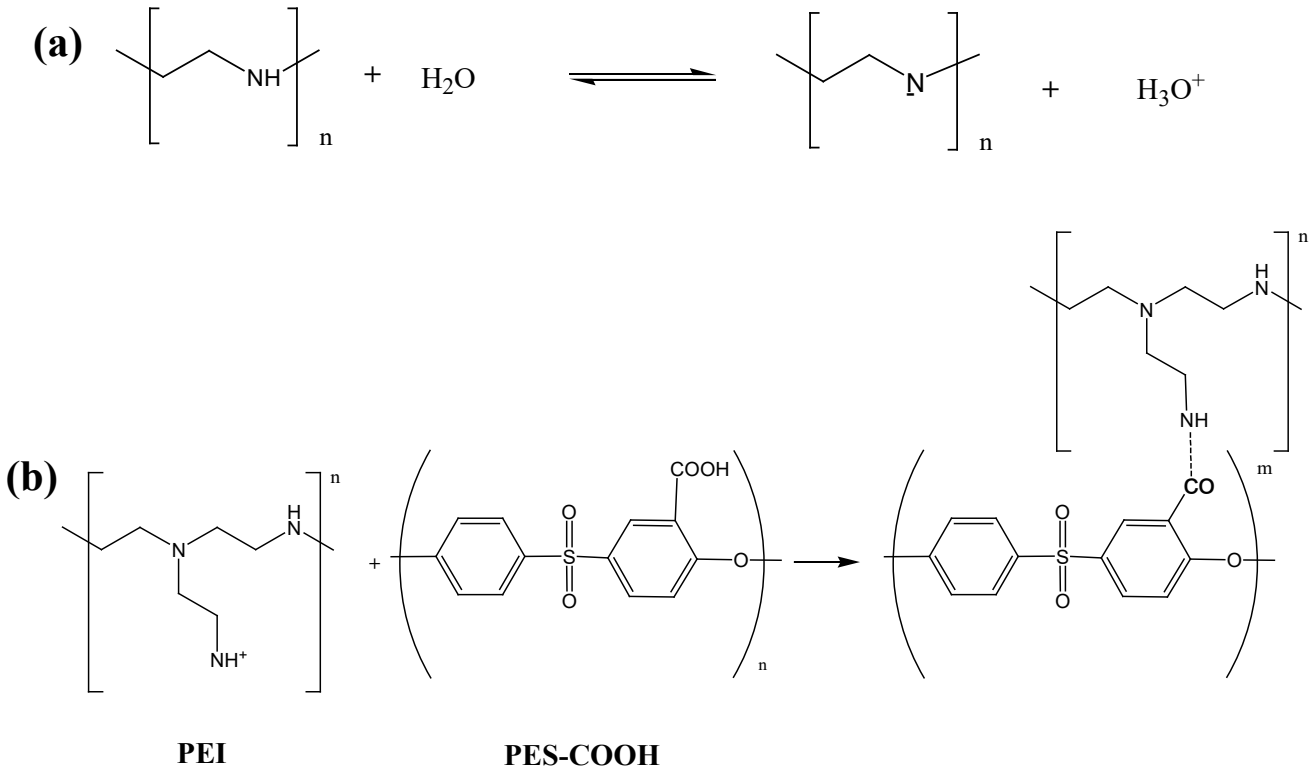


Fig. 2. Schematic of probable reactions leading to the formation of the thin-film rejection layer; a) solvation of PEI in water; b) reaction of PEI with C-PES and formation of the selective layer.

Finally, the GA solution was poured onto the formed layer to crosslink with PEI followed by

washing it with sufficient amounts of DI water to remove any unreacted reagents. An example of a final crosslinked molecule is illustrated in Fig. 3. During the crosslinking, electron pairs presented in PES-COOH also link to GA molecules and the GA molecules also react with the formed PES-COOH-PEI. By repeating the mentioned reactions, the crosslinking can be completed. As previously mentioned, GA is a monomer, which can also react with itself during crosslinking and form a dimer molecule resulting in declined positive charge of the surface as a consequence of reducing the induction of the positive charge of nitrogen [35]. Because GA is dimerized at highly alkaline pH values and high concentrations [36], the self-polymerization of GA should be prevented/reduced by controlling the pH and its concentration.

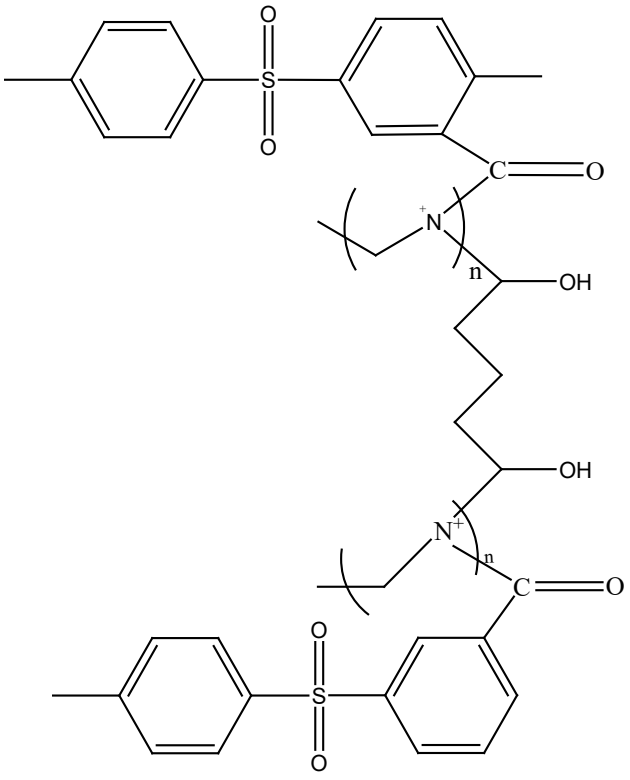


Fig. 3. Cross-linked PEI molecule.

## 2.4. Membrane characterization

Fourier transform infrared (ATR-FTIR, 8400 S) spectroscopy was employed to identify the chemical bonds of PES, C-PES, and PEI-GA-C-PES membranes.

A high-resolution field emission scanning electron microscope (FE-SEM, Mira TVLMU, TESCAN, Czech Republic) was employed to investigate the cross-section and top surface texture of the prepared TFC membranes. Membranes for cross-sectional evaluation were cast on glass, while top surface samples were cast on a polyethylene terephthalate (PET) substrate. First, the membranes were dried in a freeze-dryer, and then immersed in liquid nitrogen until they became brittle and easy to crack [37]. Later, the broken samples were sputter-coated with a very thin gold layer using a Blazers sputter coater (SCD 050, BAL-TEC, Germany) before imaging.

The contact angle of the membranes was evaluated according to the sessile drop approach using an Optical microscope (DINOLITE, model AM7915MZT, Taiwan). The prepared TFC membranes were first dried in a freeze-dryer before the measurement step. In this method, 5–7 μL of DI water were applied on the back/top surface of the membrane and the water drop profiles were then captured by a camera [38].

Water permeability of both UF and NF membranes, as well as the salt rejection of the NF membranes, were evaluated under the centration cross-flow mode using a filtration setup (Fig. 4). As illustrated, the experimental setup is equipped with a membrane cell, two pressure gauges, a temperature indicator and a rotameter, two helical heat exchangers inside the feed tank, and several valves, which provide accurate monitoring of the operating conditions. The membrane cell sample dimensions were 3 cm and 1.5 cm in length and width, respectively, providing 9 $cm^2$ of effective membrane area. All the experiments were performed under a 2.68 $m.s^{-1}$ cross-flow velocity (CFV) and 2 bar trans-membrane pressure (TMP) at 25 °C. Permeate was collected and weighed after

certain intervals to evaluate the water flux of both the UF and the NF membranes using the following equation:

$$J = \frac{m_p}{A \times \rho \times \Delta t} \quad (1)$$

where $m_p$ (kg), A ($m^2$), ρ ($kg/m^2$) and Δt (h) are mass variation over the time interval, membrane surface area, water density (equal to 1 kg/L), and a time interval, respectively. Water permeability was calculated by dividing the flux by the trans-membrane pressure.

A calibration curve with $R^2$ of 0.998 was utilized to assess the salt rejection capability of NF membranes by measuring salt passage across a membrane based on the variation of the electro conductivity (EC) employing an EC conductometer (HANNA HI 2300) and using the following equation:

$$R\ (\%) = \left(1 - \frac{C_p}{C_f}\right) \times 100 \quad (2)$$

where $R$ is the salt rejection, and $C_p$ and $C_f$ are the concentrations of salt ions in the permeate and feed streams, respectively.

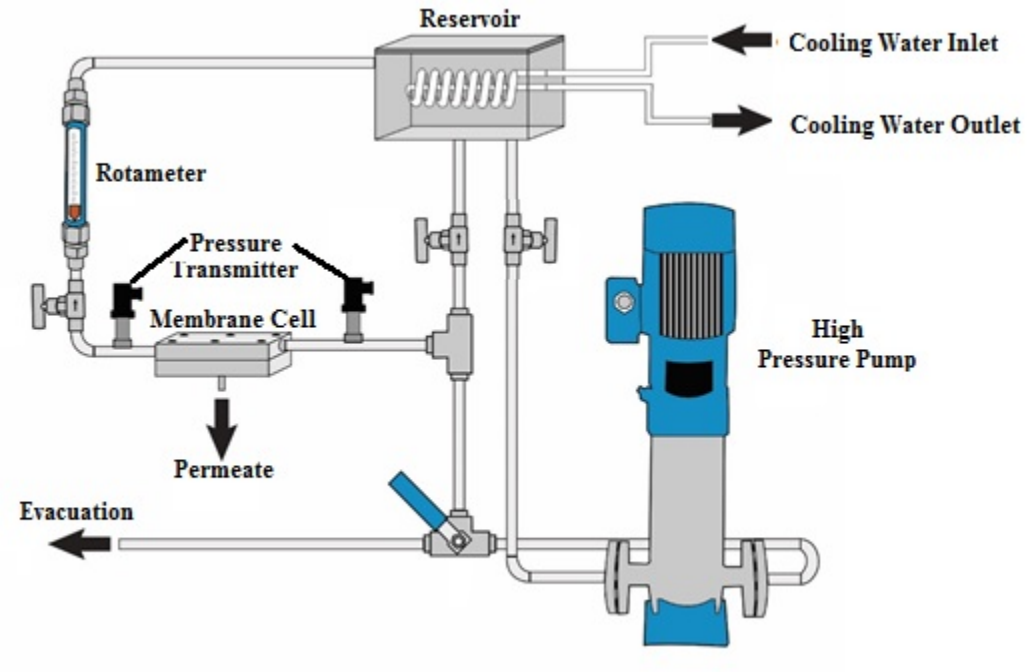


Fig. 4. Schematic of the NF experimental setup.

## 3. Results and discussions

### 3.1. Characterization of synthesized carboxylated polyethersulfone (C-PES)

As previously described in Section 2.2, C-PES was synthesized after completion of acetylation followed by the oxidation reaction of the PES polymer. FTIR and HNMR analyses were conducted to identify the formed bonds and the extent of carboxylation. Fig. 5 illustrates the FTIR spectra of the PES, PES-$COCH_3$, and C-PES powders over wavenumbers ranging from 500 $cm^{-1}$ to 4000 $cm^{-1}$. After the acetylation reaction, the band appearing at 1676 $cm^{-1}$ is assigned to the carbonyl group belonging to PES-$COCH_3$. After the oxidation reaction, two strong absorption bands appeared at 1670 $cm^{-1}$ and 3390 $cm^{-1}$, which are attributed to the stretching vibrations of the carboxylic acid functional groups. Furthermore, the bands at 2929 $cm^{-1}$ could be assigned to the –$CH_3$ stretching vibration in PES–$COCH_3$.

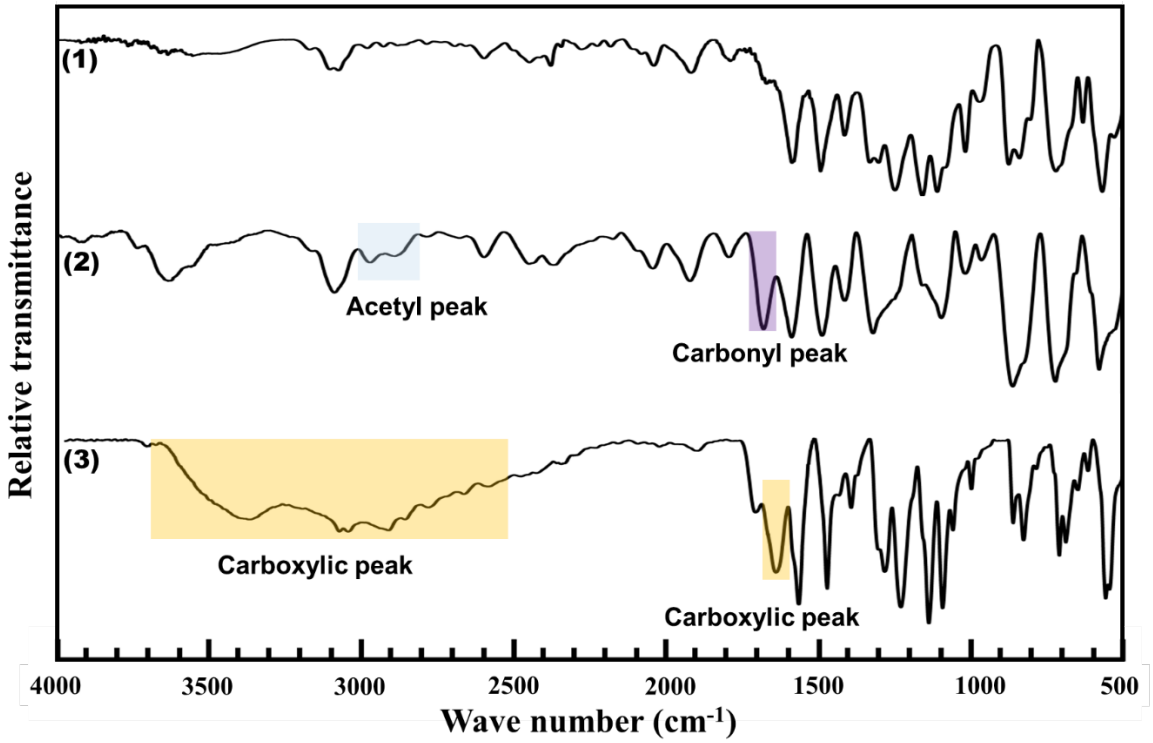


Fig.5. FTIR spectra of (1) PES, (2) PES–$COCH_3$, and (3) PES–COOH

Fig. 6 depicts the HNMR spectra of PES-$COCH_3$ and PES-COOH. The peaks at δ=7.2 and δ=7.9 in both spectra indicate the chemical shifts of the phenyl main chain of the PES. The peak at δ=2.5, denoted by the letter "b", was the chemical shift of –$COCH_3$, which was grafted onto the PES molecule after the acetylation reaction. A weak peak at 11.2, marked by the letter "c", identifies the –COOH functional group generated as a result of the oxidation reaction.

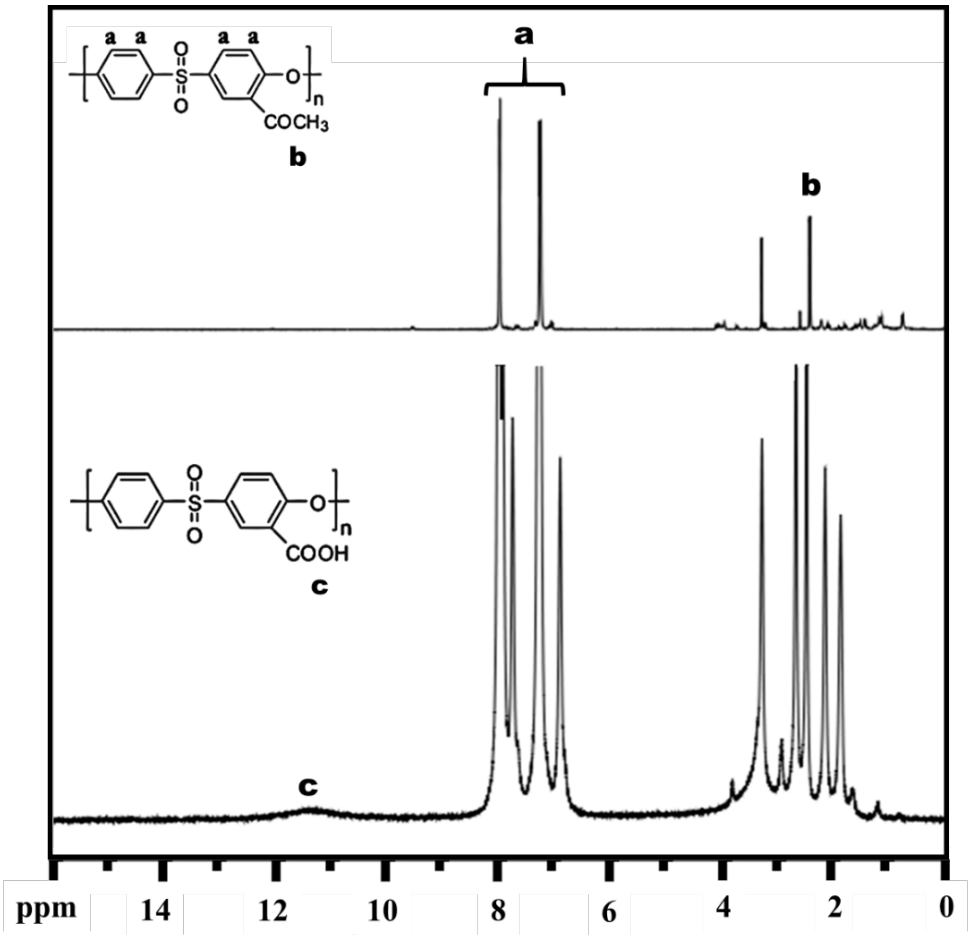


Fig. 6. HNMR spectra of PES–$COCH_3$ and PES–COOH

Both the obtained FTIR and HNMR results confirm the successful acetylation and carboxylation of PES.

### 3.2. Membrane characterizations

To investigate the chemical structure of the prepared membranes and the effect of C-PES on membrane chemical structure, ATR-FTIR measurements were carried out. Fig. 7 shows the ATR-FTIR spectrum of the C-PES net UF membrane, (C-PES)/PES blend UF membrane, and NF membrane formed on the (C-PES)/PES blend UF membrane over the wave number range of 1000–

4000 $cm^{-1}$. In Fig. 7, IR spectra 1 and 2 belong to the neat PES net UF membrane and (C-PES)/PES blend UF membrane, respectively. IR Spectrum 3 is assigned to the NF membrane prepared under the conditions of PEI concentration of 1.0 wt. %, reaction temperature of 60 °C, reaction time of 2 h, GA concentration of 0.5 wt. % and crosslinking time of 30 min. As shown in Fig. 7, the presence of the absorption bands at 1670 $cm^{-1}$ and 3429 $cm^{-1}$ is attributable to the stretching vibrations of the carboxyl functional groups (Spectrum 2). There are two bands at 1148 $cm^{-1}$ and 1238 $cm^{-1}$, which are contributed by the stretching vibrations of the tertiary amines functional group (C-N) formed during the crosslinking step, indicating the successful formation of the selective layer (Spectrum 3). Moreover, there are two other bands at 1663 $cm^{-1}$ and 3403 $cm^{-1}$ that are related to the stretching vibrations of unreacted acetyl and carboxyl functional groups, respectively, in the C-PES membrane surface.

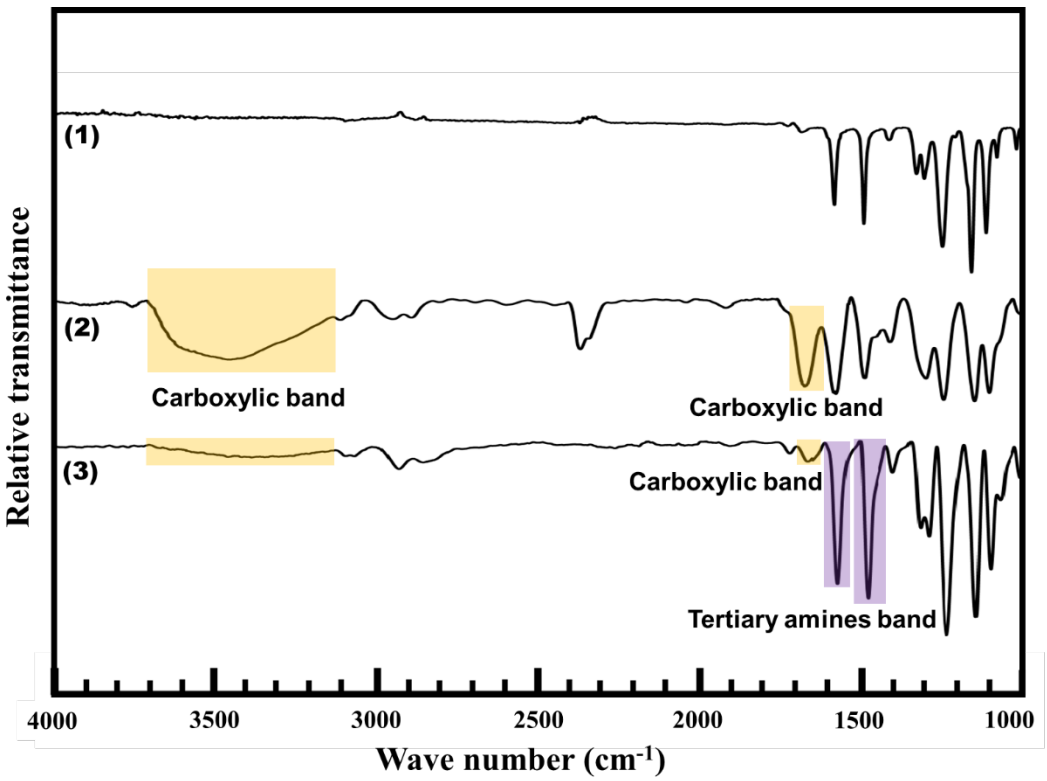


Fig. 7. ATR-FTIR spectra of 1) Neat PES UF membrane; 2) (C-PES)/PES blend UF membrane; 3) NF membrane

formed on (C-PES)/PES blend UF membrane.

As mentioned previously in Section 2.4, FE-SEM analysis was utilized to study the cross-section and top surface structure of both the UF membrane and the applied NF selective layer under the influence of C-PES addition (Fig. 8). The overall PES concentration of the dope solution in all the prepared UF membranes adjusted at 18.0 wt. % led to the formation of UF membranes with a sponge-like structure (Fig. 8(a)) [39]. As shown in Figs. 8(b) and (c), the addition of C-PES with ratio of (C-PES)/PE=1/30 and 4/30 to the dope solution resulted in the formation of finger-like structures [40]. Moreover, the surface porosity of the prepared membrane increased by increasing the C-PES concentration (Figs. 8(b′) and (c′)) because the carboxyl functional group in the C-PES is polar led to an increase in membrane hydrophilicity and faster phase separation rate [41]. Although not shown here, the contact angle decreased from 75° for the pure PES membrane to 51° for the C-PES membrane. In other words, the addition of C-PES to the dope solution can increase the solvent-nonsolvent exchange rate during phase inversion, bringing about a change of the delayed liquid-liquid separation as an instantaneous mechanism [42]. As revealed in Figs. 8(a'), (b'), and (c'), a denser top surface was obtained in the UF membrane without the addition of C-PES, while the addition of C-PES led to an increase in surface porosity as well as enlarging the mean pore size, which confirms the increased membrane hydrophilicity. Finally, after the preparation of the selective layer by employing the interfacial reaction method under the conditions of HPEI polycation aqueous solution concentration of 1.0 wt. % (pH=10.8), reaction time of 2 h, surface reaction temperature of 60 °C, GA concentration of 0.5 wt. % and cross-linking time of 30 min, an asymmetric membrane with a porous UF membrane including obvious finger-like structures was achieved (Figs. 8(d) and (e)) [43].

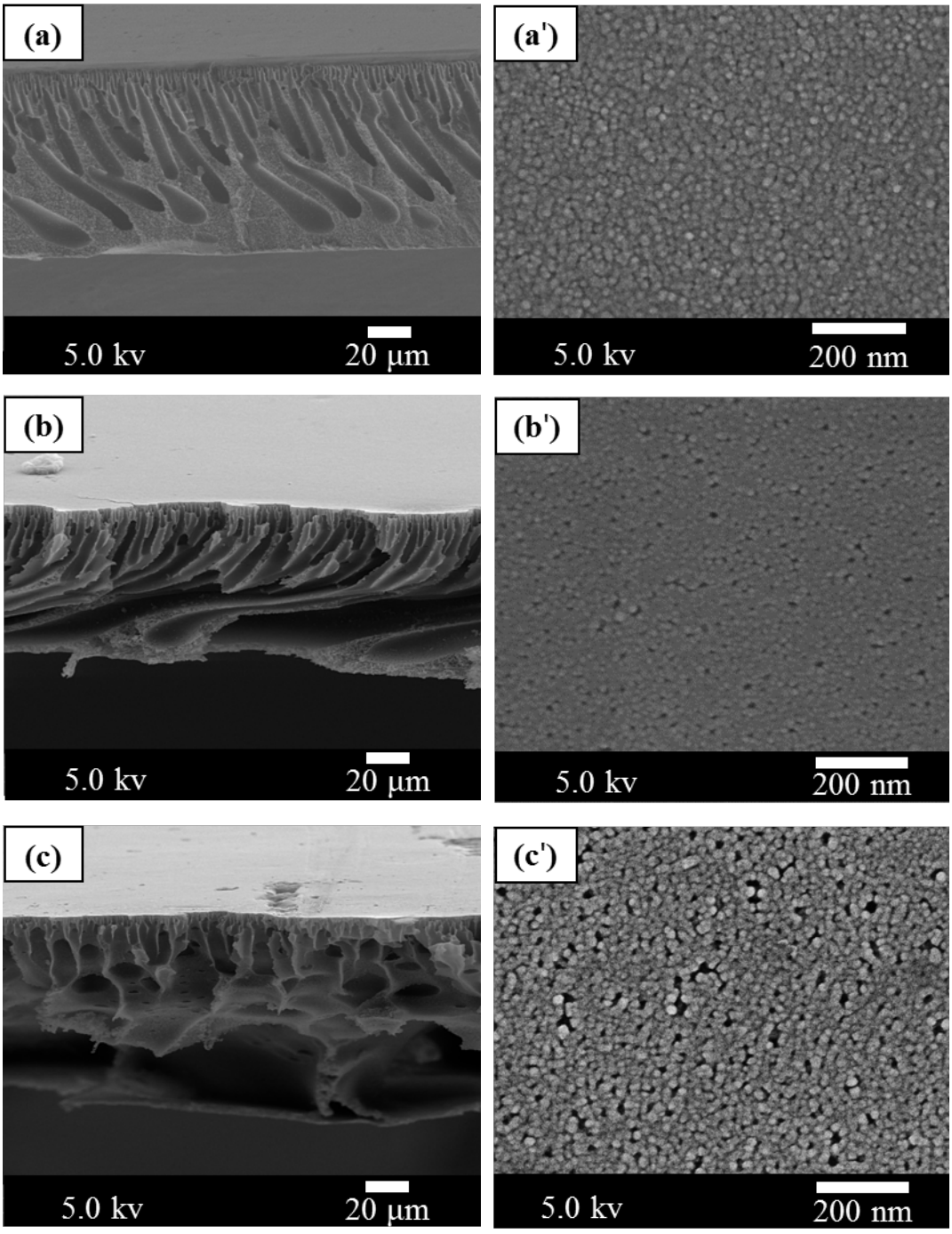
(a)
5.0 kv
20 µm
(a')
5.0 kv
200 nm
(b)
5.0 kv
20 µm
(b')
5.0 kv
200 nm
(c)
5.0 kv
20 µm
(c')
5.0 kv
200 nm

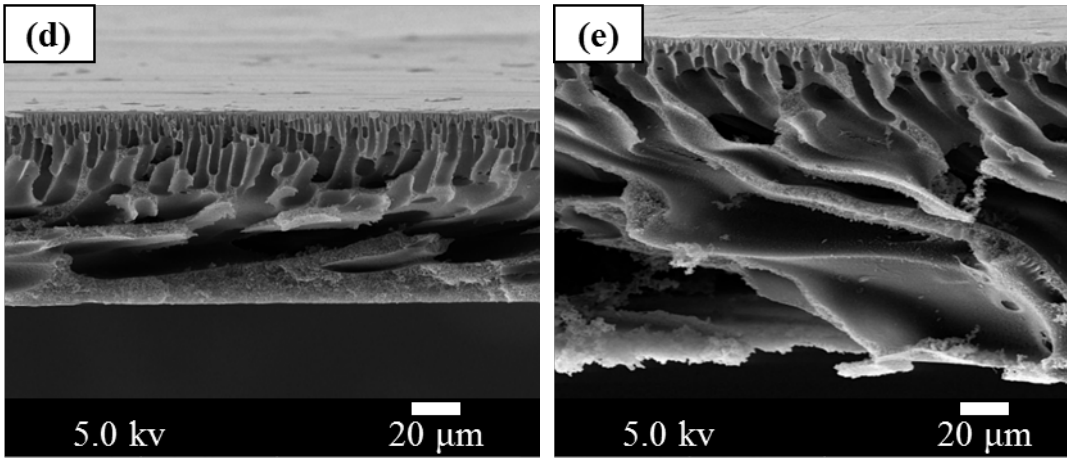


Fig. 8. FESEM cross-sectional and surface images of the prepared UF and NF membranes; Neat PES cross section and top surface (a and a' respectively); C-PES/PES=1/30 cross section and top surface (b and b' respectively); C-PES/PES=4/30 cross section and top surface (c and c' respectively); d) C-PES/PES=1/30 UF membrane and NF selective layer cross section, e) C-PES/PES= 4/30 UF membrane and NF selective layer cross section; (NF membranes: polycation concentration=1 wt. % HPEI; pH=10.8; reaction temperature=60 ˚C; reaction time=2 h; GA concentration=0.5 wt. %; cross-linking time=30 min.)

### 3.3. PES and (C-PES)/PES porous UF membrane layer performances

As mentioned previously in Section 2.3.3, the selective layer of the TFC membranes is formed on the top surface of a UF membrane. Thus, first, the water permeability performance of the (C-PES)/PES blend UF membrane was compared to a PES UF membrane with the same composition of PES, PEG-200, and DMAc. Although not shown here, the water permeability of (C-PES)/PES increased from 171 LMH/bar to approximately 248 LMH/bar (48%) owing to the increase in surface porosity as a result of C-PES addition (contact angle varied from 75° to 51°). As it is clear from Fig. 8, the addition of ~6.67% (1/15) C-PES to dope solution increased the fingerlike structures size and surface pore size.

### 3.4. Influence of kinetic parameters on TFC selective layer

### 3.4.1. Effects of membrane surface reaction temperature

One of the principal parameters affecting a reaction is obviously the reaction temperature. Thus, the impact of the reaction temperature on WP and salt rejection was investigated over the range of 10 ºC to 80 ºC by changing PEI and HPEI polycations solution temperature (surface reaction temperature). For this purpose, 1.0 wt. % of polycation aqueous solution was first subjected to the (C-PES)/PES UF membrane surface for 2 h at the given temperature. Then, the membrane was immersed in a 0.5 wt. % GA for 30 min and finally the obtained NF membrane was washed with DI water several times. As shown in Fig. 9, the WP curves of PEI and HPEI follow fairly similar trends under the influence of reaction temperature, where a sharp decline was observed as the temperature increased from 10 °C to 60 °C, with a subsequent slight increase for temperatures above 60 °C. The earlier decline of WP can be explained by the endothermic nature of the reaction of PEI with C-PES (which provides a denser selective layer). The observed increment can be attributed to breaking NH-CO bonds on the surface of the selective layer with increasing temperature. Accordingly, the nitrogen in the amine group in the PEI structure absorbs $H_3O^+$ because it contains non-bonding pairs of electrons. As a result, ammonium cations ($NH_4^+$) are formed, leading to breaking of the bonds between the carboxyl and amine groups. Consequently, the pore size increases [44, 45].

Concerning salt rejection, the trends undergo a different scenario, in which rejection increased as the temperature was raised to 40 °C and 60 °C for PEI and HPEI, respectively, followed by a slight decline. Moreover, application of HPEI exhibited higher salt rejection compared to PEI application. This can be attributed to the presence of a greater number of positive charges on the membrane selective layer, which enhance ion repletion and reduce concentration polarization [21].

389 Overall, it can be observed that utilizing HPEI induces better performance in terms of WP and salt
390 rejection compared to PEI under the influence of the reaction temperature.

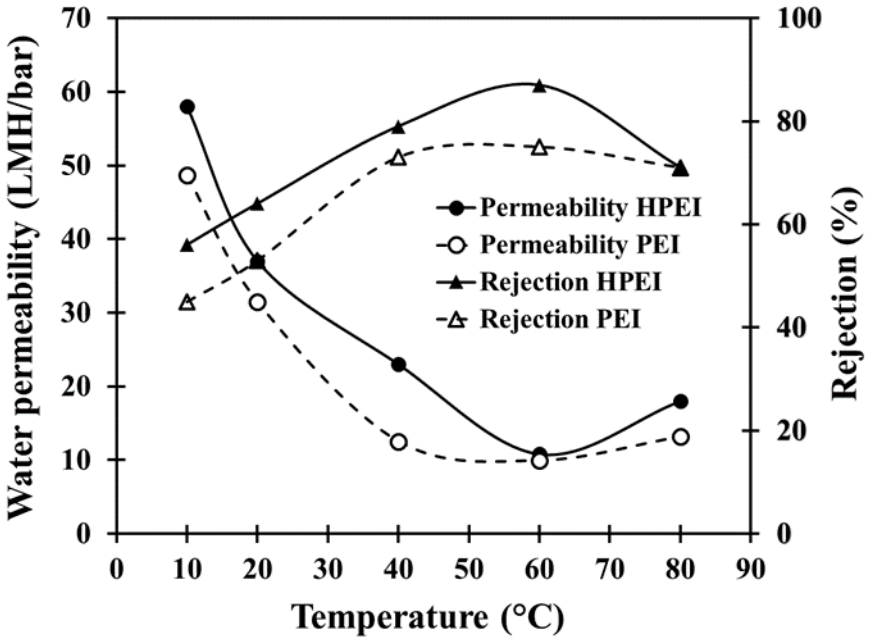


391

392 Fig. 9. Effects of reaction temperature on water permeability and $MgCl_2$ (1000 mg/L) rejection. (UF membrane
393 polymer concentration=18 wt. %; (C-PES)/PES=1/15; polycation concentration =1 wt. % PEI/HPEI; pH=10.8;
394 reaction time=2 h; GA concentration=0.5 wt. %; cross-linking time=30 min; operating pressure=2 bar).

395

396 **3.4.2. Effects of surface reaction and crosslinking times**

397 To investigate the effects of surface reaction and crosslinking times on WP and salt rejection,
398 a similar approach to that was mentioned in the Section 3.3.1 was applied to prepare NF membrane.
399 The only difference was that the surface reaction temperature was fixed at 60 °C and the surface
400 reaction time was varied from a few minutes to 24 h. Also, the crosslinking reaction time was
401 changed from 10- 40 min. The sharp decline of WP in the first 2 hours indicates a higher portion
402 of reacted PEI or HPEI on the membrane surface [26]. The reason is related to the increasing the

positive charge density of the reaction medium which in turn significantly increases the electrostatic attraction force between the amine groups of the PEI/HPEI and negatively-charged carboxyl groups of the membrane surface. By further increasing the surface reaction time, more $H_3O^+$ species release which decreases the pH of the reaction medium. As the result, a few surface reactions occur between PEI and the UF membrane. This will be discussed in more details in Section 3.4.4. A similar rationale is also valid in explaining the rejection trends. The crosslinking reaction time was also evaluated after optimizing the membrane surface reaction time (Fig. 10(b)). WP declined as the crosslinking time increased to approximately 30 min. However, an ascending trend was observed after 30 min. Also, an oppose trend was observed for the rejection results over whole time range. This might be explained by the dimerization of GA as a result of providing sufficiently long reaction times, which could increase the interspace of the selective layer [26].

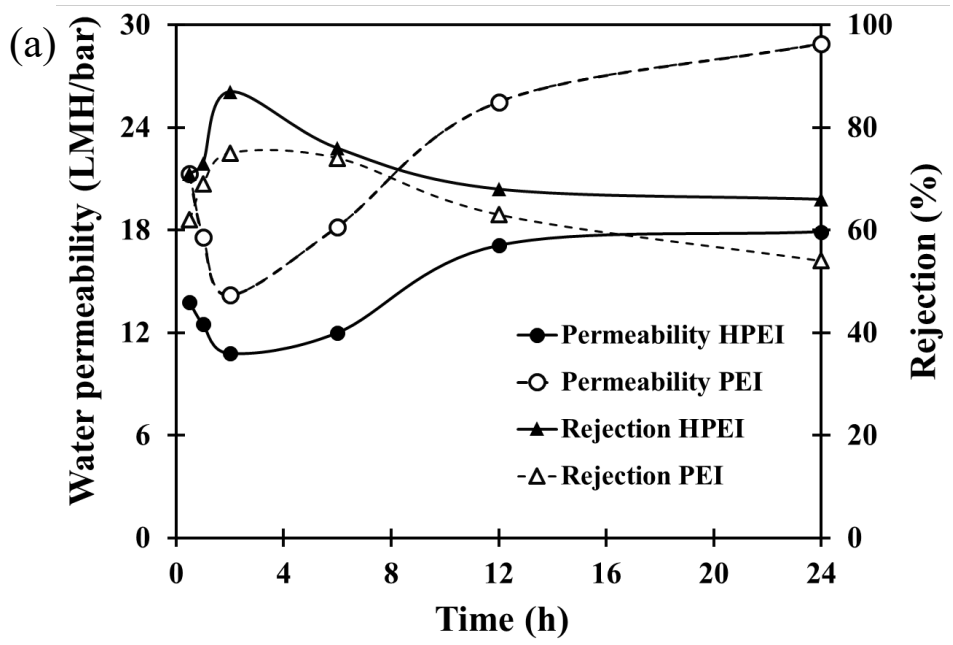

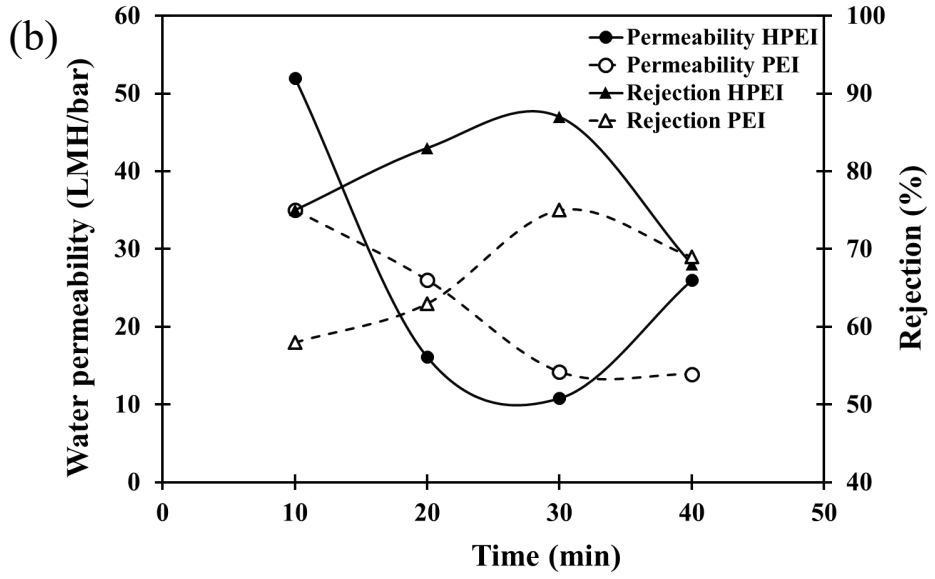


414 Fig. 10. Effects of a) Surface reaction and b) crosslinking time on water permeability and $MgCl_2$ (1000 mg/L)
415 rejection of the TFC NF membrane. (UF membrane polymer concentration=18 wt. %; (C-PES)/PES=1/15;
416 polycation concentration=1 wt. % PEI/HPEI; pH=10.8; reaction temperature=60 °C; GA concentration=0.5 wt. %;
417 operating pressure=2 bar; for a: cross-linking time=30 min; for b: reaction time=2 h)

418

419 **3.4.3. Effects of PEI/HPEI and GA concentrations on the performance of the TFC NF**
420 **membrane**

421 To evaluate the effects of polycation and GA concentrations on the performance of TFC NF
422 membranes, the approach previously described in Section 3.4.1 was applied. Accordingly, surface
423 and crosslinking reaction times were set at 2 h and 30 min, respectively. Also, the surface reaction
424 temperature was fixed at 60 °C temperature. The polycations solution concentration was varied
425 from 0.1 to 5 wt. %. As depicted in Fig. 11(a), salt rejection of the membrane increased as the
426 concentration of both PEI and HPEI was raised from 0.1 to 1.0 wt. %, while a slight enhancement
427 was observed by further increasing the polycations concentration. This can be attributed to the
428 presence of limited amounts of C-PES functional groups on the top surface of the prepared UF

blend membrane. In other words, the surface C-PES will react with the introduced polycation molecules until no C-PES molecules remain unreacted. Thus, extra PEI/HPEI molecules remain in the reaction medium without involvement in the reactions. Fig. 11(b) shows the effect of GA concentration on WP and $MgCl_2$ (1000 mg/L) rejection for the TFC NF membranes. As can be clearly seen, the rejection increases with the increase of GA concentration up to 0.5 wt. % and thereafter experiences a declining trend. This is evidently opposite to WP. At GA concentrations of less than 0.5 wt. %, GA cross-links the PEI branches and this reduces the pore size and eventually increases rejection. At GA concentrations greater than 0.5 wt. %, the dimerization of GA occurs, resulting in reduced crosslinking between PES-COOH and PEI. This in turn reduces the positive charge of the surface. Furthermore, increasing the length of the GA chain through dimerization can increase the free volume in the polymeric structure and suppress the rejection [35, 36].

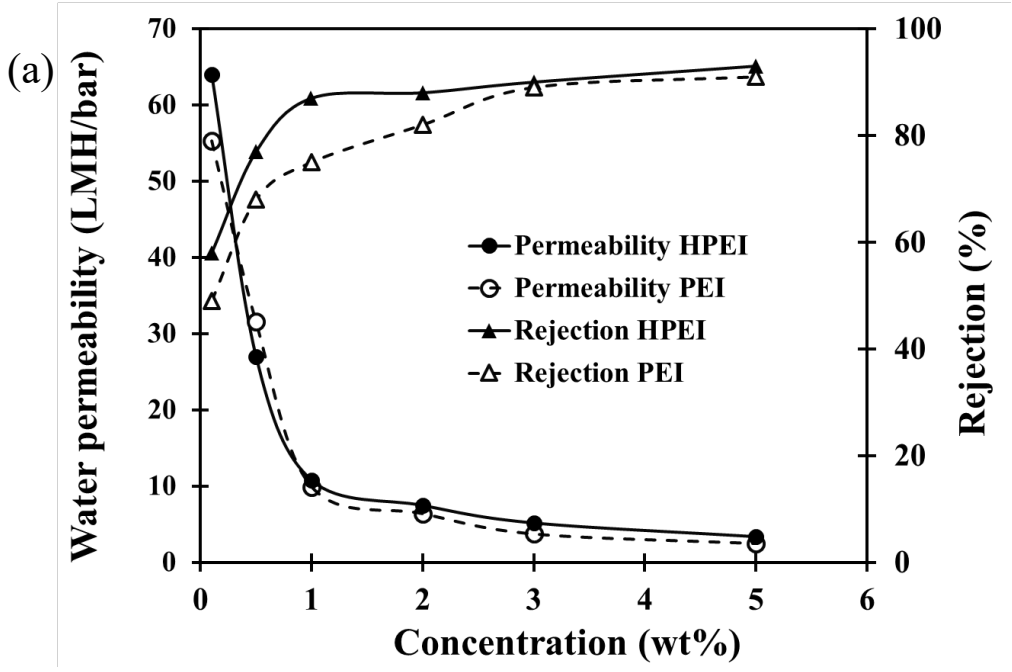

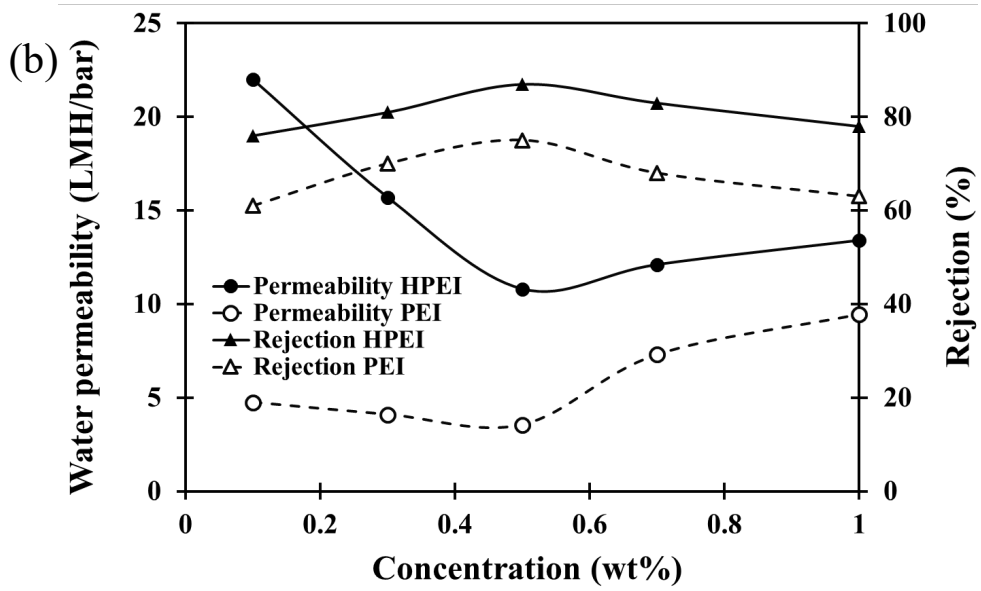


441 a) Fig. 11. Effects of a) PEI and HPEI, and b) GA concentrations on water permeability and $MgCl_2$ (1000
442 mg/L) rejection of the TFC NF membrane. (UF membrane polymer concentration=18 wt. %; (C-
443 PES)/PES=1/15; reaction time=2 h; reaction temperature=60 °C; cross-linking time=30 min; operating
444 pressure=2 bar; for a: GA concentration=0.5 wt. %; for b: polycation concentration=1 wt. % PEI/HPEI)

445

446 **3.4.4. Effects of pH of the PEI/HPEI solution on the performance of the TFC NF**
447 **membrane**

448 To study the effect of pH of the PEI/HPEI solution on the performance of the TFC NF
449 membranes, the overall preparation steps which were explained in Section 3.4.1. were used to
450 fabricate the NF membranes. The initial pH value of PEI/HPEI was 10.8. The surface reaction
451 temperature and time were 60 °C and 2 h, respectively. The crosslinking reaction was performed
452 utilizing 0.5 wt. % GA for 30 min. The pH value of PEI/HPEI solution was varied from 5 to 12.
453 The effects of the pH of the PEI and HPEI solutions on the performance of TFC nano-filtration
454 membranes were examined and the results are illustrated in Fig. 12.

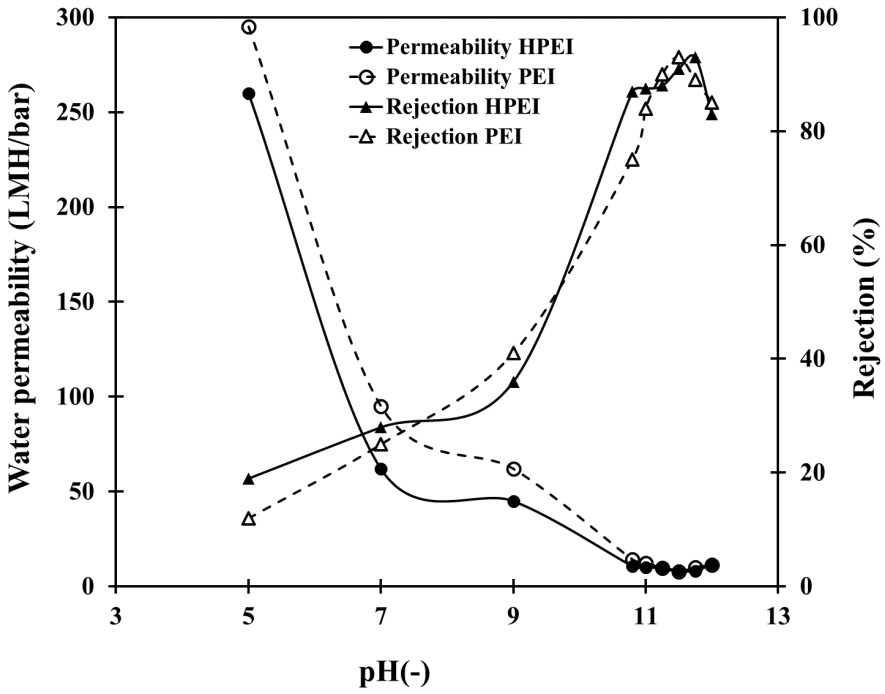


455

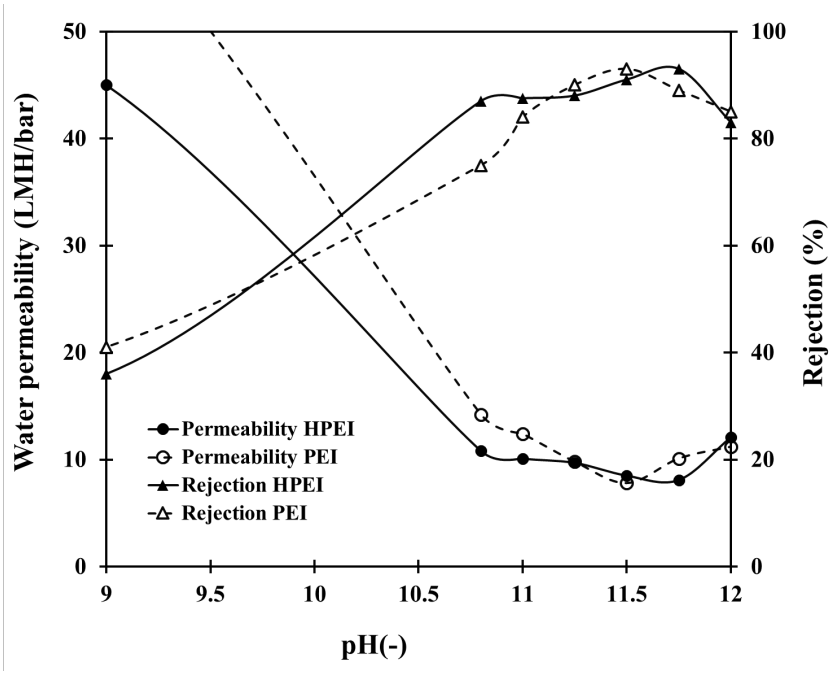


456

457 Fig. 12. Effects of pH values of PEI and HPEI solutions on water permeability and $MgCl_2$ (1000 mg/L) rejection of
458 the TFC NF membrane. Top: total pH range studied; Bottom: alkaline pH range with more obvious details. (UF
459 membrane polymer concentration=18 wt. %; (C-PES)/PES=1/15; polycation concentration=1 wt. % PEI/HPEI;

460 reaction time=2 h; reaction temperature=60 °C; GA concentration=0.5 wt. %; cross-linking time=30 min; operating
461 pressure=2 bar)

462

463 From Fig. 12, at low pH, water permeability is high with very low $Mg^{2+}$ rejection. The results
464 indicate that the optimal pH values of HPEI and PEI solutions are 10.75 and 11.50, respectively,
465 with the highest $Mg^{2+}$ rejection of 93% achieved for both solutions. In addition, at the optimal pH
466 values of the HPEI and PEI solutions, water permeability values of approximately 8.1 LMH/bar
467 and 7.8 LMH/bar are observed, respectively. In addition, by further increasing the pH up to 12, a
468 drop in membrane rejection is observed with a jump in water permeability. This behavior at
469 different pH values can be explained as follows:

470 At acidic pH values, both PEI and HPEI are partially or entirely protonated (at acidic pH values,
471 the PEI protonation degree is ~45% [46]).. The PEI was reported to be positively charged at pH
472 values below its isoelectric point of 9.8 owing to the protonation of the amine functional groups
473 [47]. The electrostatic repulsion between protonated amine groups induces expansion of the
474 polymer chains, which leads to the "openness" of the membrane pores and increases the membrane
475 pore size [48, 49]. Additionally, at low pH values, only a few surface reactions occur between PEI
476 and the membrane support layer. By increasing the solution pH to 7, the protonation extent of the
477 amine groups of PEI is diminished to ~20% [46], and thus the pore size experiences a decline
478 owing to the reduced electrostatic repulsion interaction. Increasing the pH value up to 11.50, the
479 carboxyl groups of the support layer are partially protonated and exhibit a more extended
480 conformation [50, 51]. This in turn leads to a surface reaction between the negatively charged PEI
481 and the membrane surface functional groups, owing to the electrostatic attraction forces. Such a
482 reaction decreases the membrane pore size. Furthermore, hydrogen bonds are established between

un-deprotonated PEI species. An alternative explanation based on the electroviscous effect as a physical phenomenon exists [52]. The electroviscous effect takes place when an electrolyte solution is pressed through a narrow capillary or pore with charged surfaces. The membrane permeability decreases because the induced streaming potential exerts an electrical stress (extra drag) on the fluid. The electroviscous effect increases as the membrane charge increases. These effects increase and decrease the rejection and permeability, respectively. However, a completely different mechanism exists at the pH values higher than 11.50 and is related to the stability of the PEI structure at various pH values. PEI contains primary, secondary, and tertiary amine groups in varying ratios, which deprotonate at various pH values [53]. At pH values higher than 11.50, the amine functional groups of PEI are deprotonated. The released protons are absorbed by $OH^-$ species, resulting in the –COOH groups not being ionized. As a result, very few reactions between the –COOH groups and PEI occur, leading to the formation of large pores. This brings about an increase in water permeability and a decrease in the rejection of the membrane.

As can clearly be seen in Fig. 12, PEI induces higher permeability compared to HPEI throughout the pH range. This is more likely due to the smaller surface charge density and lower thickness of the selective layer because of the linear PEI, while HPEI induces a larger surface charge density and higher thickness of the selective layer.

### 3.4.5. Influence of adding polyelectrolyte solution on the TFC NF membrane performance

Adding salt to the polycationic solution can decrease the electrostatic repulsion of the polymer chains and also alter the ionic strength of the deposition solution. This leads to the adsorption of the polymer chain as coil conformation rather than flat conformation [54, 55].

To investigate the influence of adding polyelectrolyte solution (aqueous NaCl) on the TFC NF membrane performance, some PEI solutions containing different NaCl concentrations (0-3.5

506 mol/L) were prepared. The experimental conditions: PEI/HPEI concentration, reaction
507 temperature, reaction time, GA concentration, and crosslinking time were fixed at 1.0 wt. %, 60 °C,
508 2 h, 0.5 wt. %, and 30 min, respectively. The results are shown in Fig. 13. Two different trends
509 can be observed in Fig. 13. First, the WP and salt rejection of the TFC NF membrane exhibited a
510 continuous decrease and increase, respectively as the NaCl concentration was increased up to 2.5
511 mol/L, and thereafter, a reverse trend was observed. The reason for the first trend is related to the
512 increased $Cl^-$ concentration within the reaction medium, which drives the membrane surface
513 reaction into side-reactions. In other words, excess $Cl^-$ within the reaction medium pushes the C-
514 PES-PEI reaction backward and decomposes the formed rejection layer. However, further increase
515 in the NaCl concentration (above 2.5 mol/L) screens the electrostatic repulsion, and the behavior
516 of the solution resembles that of neutral polymers [45, 56]. As a result, a large portion of carboxyl
517 groups and PEI remains unreacted, resulting in the formation of larger pore size. In addition, such
518 a two-face trend is related to the protonation degree of PEI or HPEI in the presence of chloride
519 ions. According to the literature, the protonation degree of PEI is affected by the presence of
520 chloride ions. The activity coefficient of chloride ions (as counterions) in a polyelectrolyte solution
521 is lower than that in a simple salt solution at the same concentration. A polyelectrolyte solution
522 such as a PEI or HPEI solution, which has a large charge density, induces a strong interaction
523 between the polyelectrolyte and the counterions (chloride ions) [57].

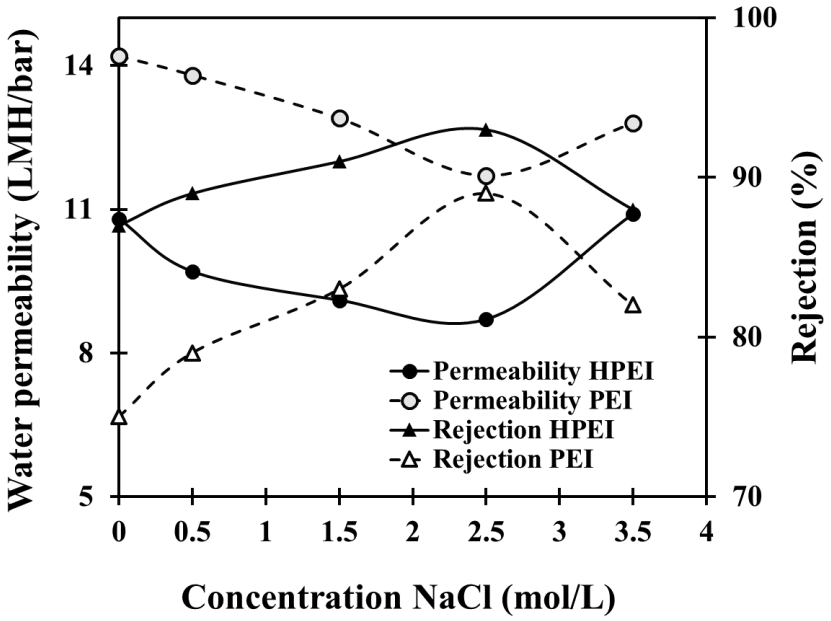


524

525 Fig. 13. Effect of NaCl addition on water permeability and $MgCl_2$ (1000 mg/L) rejection of the TFC NF membrane.
526 (UF membrane polymer concentration=18 wt. %; (C-PES)/PES=1/15; polycation concentration=1 wt. % PEI/HPEI;
527 pH=10.8; reaction time=2h; reaction temperature=60 °C; GA concentration=0.5 wt. %; cross-linking time=30 min;
528 operating pressure=2 bar)

529 Compared to when NaOH was added to the reaction medium, NaCl addition has a milder effect
530 on the TFC NF membrane, because $Cl^-$ is a weaker base ion compared to $OH^-$. However, it provides
531 better conditions for the forward membrane surface reactions compared to the conditions without
532 adding basic chemicals.

533 ## 4. Conclusion

534 The membrane surface reaction was exploited to obtain a TFC membrane for low-pressure NF
535 water softening applications. (C-PES)/PES blend UF membranes were first fabricated, and
536 subsequently, PEI and HPEI reacted with the surface blend carboxyl functional groups group
537 to produce TFC nano-filtration membranes. Addition of a small amount of C-PES to the dope
538 solution drastically affected the blend UF membrane characteristics, including membrane

structure, water permeability and salt rejection. Optimized reaction time, PEI solution concentration, cross-linking time, cross-linking agent, and supporting polyelectrolyte are needed to obtain the maximum water filtration performance (WP and rejection) of the TFC NF membrane. The pH of the PEI solution had a drastic effect on the prepared TFC NF membranes. TFC NF membrane water filtration performance was explained based on the single reaction (between C-PES and PEI) and polymer chemistry mechanism. After optimizing the preparathion condition, a membrane with WP as high as 10.1 LMH/bar and $MgCl_2$ (1000 ppm) rejection of 90% was obtained.

**Acknowledgment**

The authors would like to express their appreciation to the Iran National Science Foundation (INSF: grant number 96008182) and Iran Fuel Conservation Company (IFCO) for supporting this research.

**References**

[1] C. Schmitz, H. Lotze-Campen, D. Gerten, J.P. Dietrich, B. Bodirsky, A. Biewald, A. Popp, Blue water scarcity and the economic impacts of future agricultural trade and demand, Water Resour. Res. 49 (2013) 3601-3617 https://doi.org/10.1002/wrcr.20188.

[2] P.H. Gleick, N.L. Cain, The world's water 2004-2005: the biennial report on freshwater resources, Island Press, 2004.

[3] M. Schiffler, Perspectives and challenges for desalination in the 21st century, Desalination 165 (2004) 1-9 https://doi.org/10.1016/j.desal.2004.06.001.

559 [4] C. Fritzmann, J. Löwenberg, T. Wintgens, T. Melin, State-of-the-art of reverse osmosis
560 desalination, Desalination 216 (2007) 1-76 https://doi.org/10.1016/j.desal.2006.12.009.

561 [5] A.M. Hanra, V. Ramachandhran, RO performance analysis of cellulose acetate and TFC
562 polyamide membrane systems for separation of trace contaminants, Desalination 104 (1996) 175-
563 183 https://doi.org/10.1016/0011-9164(96)00040-9.

564 [6] J. Lv, K.Y. Wang, T.-S. Chung, Investigation of amphoteric polybenzimidazole (PBI)
565 nanofiltration hollow fiber membrane for both cation and anions removal, J. Membr. Sci. 310
566 (2008) 557-566 https://doi.org/10.1016/j.memsci.2007.11.050.

567 [7] Y. Fernández-Torquemada, J.M. Gónzalez-Correa, A. Loya, L.M. Ferrero, M. Díaz-Valdés,
568 J.L. Sánchez-Lizaso, Dispersion of brine discharge from seawater reverse osmosis desalination
569 plants, Desalin. Water Treat. 5 (2009) 137-145 https://doi.org/10.5004/dwt.2009.576.

570 [8] J. Hofman, E. Beerendonk, H. Folmer, J. Kruithof, Removal of pesticides and other
571 micropollutants with cellulose-acetate, polyamide and ultra-low pressure reverse osmosis
572 membranes, Desalination 113 (1997) 209-214 https://doi.org/10.1016/S0011-9164(97)00131-8.

573 [9] A.W. Mohammad, Y. Teow, W. Ang, Y. Chung, D. Oatley-Radcliffe, N. Hilal, Nanofiltration
574 membranes review: Recent advances and future prospects, Desalination 356 (2015) 226-254
575 https://doi.org/10.1016/j.desal.2014.10.043.

576 [10] Y. Song, T. Li, J. Zhou, Z. Li, C. Gao, Analysis of nanofiltration membrane performance
577 during softening process of simulated brackish groundwater, Desalination 399 (2016) 159-164
578 https://doi.org/10.1016/j.desal.2016.09.004.

[11] J. Shen, A.I. Schäfer, Factors affecting fluoride and natural organic matter (NOM) removal from natural waters in Tanzania by nanofiltration/reverse osmosis, Sci. Total Environ. 527 (2015) 520-529 https://doi.org/10.1016/j.scitotenv.2015.04.037.

[12] B. Van der Bruggen, Nanofiltration, Encyclopedia of Membrane Science and Technology (2013) 1-23 https://doi.org/10.1002/9781118522318.emst077.

[13] S. Chou, R. Wang, L. Shi, Q. She, C. Tang, A.G. Fane, Thin-film composite hollow fiber membranes for pressure retarded osmosis (PRO) process with high power density, J. Membr. Sci. 389 (2012) 25-33 https://doi.org/10.1016/j.memsci.2011.10.002.

[14] D.L. Oatley-Radcliffe, M. Walters, T.J. Ainscough, P.M. Williams, A.W. Mohammad, N. Hilal, Nanofiltration membranes and processes: A review of research trends over the past decade, J. Water Proc. Eng. 19 (2017) 164-171 https://doi.org/10.1016/j.jwpe.2017.07.026.

[15] A. Simon, W.E. Price, L.D. Nghiem, Changes in surface properties and separation efficiency of a nanofiltration membrane after repeated fouling and chemical cleaning cycles, Sep. Purif. Technol. 113 (2013) 42-50 https://doi.org/10.1016/j.seppur.2013.04.011.

[16] Y. Song, W. Qin, T. Li, Q. Hu, C. Gao, The role of nanofiltration membrane surface charge on the scale-prone ions concentration polarization for low or medium saline water softening, Desalination 432 (2018) 81-88 https://doi.org/10.1016/j.desal.2018.01.013.

[17] A.E. Childress, M. Elimelech, Effect of solution chemistry on the surface charge of polymeric reverse osmosis and nanofiltration membranes, J. Membr. Sci. 119 (1996) 253-268 https://doi.org/10.1016/0376-7388 (96)00127-5.

[18] B. Al-Rashdi, C. Somerfield, N. Hilal, Heavy metals removal using adsorption and nanofiltration techniques, Sep. Purif. Rev. 40 (2011) 209-259 https://doi.org/10.1080/15422119.2011.558165.

[19] T.A. Kurniawan, G.Y. Chan, W.-H. Lo, S. Babel, Physico–chemical treatment techniques for wastewater laden with heavy metals, Chem. Eng. J. 118 (2006) 83-98 https://doi.org/10.1016/j.cej.2006.01.015.

[20] K.Y. Wang, T.S. Chung, Polybenzimidazole nanofiltration hollow fiber for cephalexin separation, AIChE j. 52 (2006) 1363-1377 https://doi.org/10.1002/aic.10741.

[21] W. Fang, L. Shi, R. Wang, Interfacially polymerized composite nanofiltration hollow fiber membranes for low-pressure water softening, J. Membr. Sci. 430 (2013) 129-139 https://doi.org/10.1016/j.memsci.2012.12.011.

[22] R. Zhang, Y. Su, X. Zhao, Y. Li, J. Zhao, Z. Jiang, A novel positively charged composite nanofiltration membrane prepared by bio-inspired adhesion of polydopamine and surface grafting of poly (ethylene imine), J. Membr. Sci. 470 (2014) 9-17 https://doi.org/10.1016/j.memsci.2014.07.006.

[23] L. Setiawan, L. Shi, R. Wang, Dual layer composite nanofiltration hollow fiber membranes for low-pressure water softening, Polymer 55 (2014) 1367-1374 https://doi.org/10.1016/j.polymer.2013.12.032.

[24] W. Fang, L. Shi, R. Wang, Mixed polyamide-based composite nanofiltration hollow fiber membranes with improved low-pressure water softening capability, J. Membr. Sci. 468 (2014) 52-61 https://doi.org/10.1016/j.memsci.2014.05.047.

620 [25] S. Rajabzadeh, C. Liu, L. Shi, R. Wang, Preparation of low-pressure water softening hollow
621 fiber membranes by polyelectrolyte deposition with two bilayers, Desalination 344 (2014) 64-70
622 https://doi.org/10.1016/j.desal.2014.03.013.

623 [26] C. Liu, L. Shi, R. Wang, Crosslinked layer-by-layer polyelectrolyte nanofiltration hollow
624 fiber membrane for low-pressure water softening with the presence of SO42− in feed water, J.
625 Membr. Sci. 486 (2015) 169-176 https://doi.org/10.1016/j.memsci.2015.03.050.

626 [27] C.V. Gherasim, T. Luelf, H. Roth, M. Wessling, Dual-charged hollow fiber membranes for
627 low-pressure nanofiltration based on polyelectrolyte complexes: one-step fabrication with tailored
628 functionalities, ACS Appl. Mater. 8 (2016) 19145-19157 https://doi.org/10.1021/acsami.6b05706.

629 [28] S.K. Lim, L. Setiawan, T.-H. Bae, R. Wang, Polyamide-imide hollow fiber membranes
630 crosslinked with amine-appended inorganic networks for application in solvent-resistant
631 nanofiltration under low operating pressure, J. Membr. Sci. 501 (2016) 152-160
632 https://doi.org/10.1016/j.memsci.2015.11.016.

633 [29] X. Li, C. Zhao, M. Yang, B. Yang, D. Hou, T. Wang, Reduced graphene oxide-NH2 modified
634 low pressure nanofiltration composite hollow fiber membranes with improved water flux and
635 antifouling capabilities, Appl. Surf. Sci. 419 (2017) 418-428
636 https://doi.org/10.1016/j.apsusc.2017.04.080.

637 [30] D. Wang, W. Zou, L. Li, Q. Wei, S. Sun, C. Zhao, Preparation and characterization of
638 functional carboxylic polyethersulfone membrane, J. Membr. Sci. 374 (2011) 93-101
639 https://doi.org/10.1016/j.memsci.2011.03.021.

[31] H. Salehi, A. Shakeri, M. Rastgar, Carboxylic polyethersulfone: A novel pH-responsive modifier in support layer of forward osmosis membrane, J. Membr. Sci. 548 (2018) 641-653 https://doi.org/10.1016/j.memsci.2017.10.044.

[32] E. Saljoughi, M. Sadrzadeh, T. Mohammadi, Effect of preparation variables on morphology and pure water permeation flux through asymmetric cellulose acetate membranes, J. Membr. Sci. 326 (2009) 627-634 https://doi.org/10.1016/j.memsci.2008.10.044.

[33] M. Amirilargani, A. Sabetghadam, T. Mohammadi, Polyethersulfone/polyacrylonitrile blend ultrafiltration membranes with different molecular weight of polyethylene glycol: preparation, morphology and antifouling properties, Polym. Adv. Technol. 23 (2012) 398-407 https://doi.org/10.1002/pat.1888.

[34] T. Okubo, N. Ise, Studies on Carbamoylation Reactions of Polyethylenimine and Its Low Molecular Weight Analogues with Cyanate Ions, Bull. Chem. Soc. Jpn. 46 (1973) 2493-2497 https://doi.org/10.1246/bcsj.46.2493.

[35] L. Betancor, F. López-Gallego, A. Hidalgo, N. Alonso-Morales, G.D.-O.C. Mateo, R. Fernández-Lafuente, J.M. Guisán, Different mechanisms of protein immobilization on glutaraldehyde activated supports: effect of support activation and immobilization conditions, Enzyme Microb. Technol. 39 (2006) 877-882 https://doi.org/10.1016/j.enzmictec.2006.01.014.

[36] I. Migneault, C. Dartiguenave, M.J. Bertrand, K.C. Waldron, Glutaraldehyde: behavior in aqueous solution, reaction with proteins, and application to enzyme crosslinking, Biotechniques 37 (2004) 790-802 https://doi.org/10.2144/04375RV01.

660 [37] D.R. Lloyd, K.E. Kinzer, H. Tseng, Microporous membrane formation via thermally induced
661 phase separation. I. Solid-liquid phase separation, J. Membr. Sci. 52 (1990) 239-261
662 https://doi.org/10.1016/S0376-7388 (00)85130-3.

663 [38] P. Shen, A. Moriya, S. Rajabzadeh, T. Maruyama, H. Matsuyama, Improvement of the
664 antifouling properties of poly (lactic acid) hollow fiber membranes with poly (lactic acid)–
665 polyethylene glycol–poly (lactic acid) copolymers, Desalination 325 (2013) 37-39
666 https://doi.org/10.1016/j.desal.2013.06.012.

667 [39] I.-C. Kim, K.-H. Lee, T.-M. Tak, Preparation and characterization of integrally skinned
668 uncharged polyetherimide asymmetric nanofiltration membrane, J. Membr. Sci. 183 (2001) 235-
669 247 https://doi.org/10.1016/S0376-7388 (00)00588-3.

670 [40] J. Hester, A. Mayes, Design and performance of foul-resistant poly (vinylidene fluoride)
671 membranes prepared in a single-step by surface segregation, J. Membr. Sci. 202 (2002) 119-135
672 https://doi.org/10.1016/S0376-7388 (01)00735-9.

673 [41] S. Rimmer, S. Carter, R. Rutkaite, J.W. Haycock, L. Swanson, Highly branched poly-(N-
674 isopropylacrylamide) s with arginine–glycine–aspartic acid (RGD)-or COOH-chain ends that form
675 sub-micron stimulus-responsive particles above the critical solution temperature, Soft Matter 3
676 (2007) 971-973 https://doi.org/10.1039/B705188C.

677 [42] V. Vatanpour, S.S. Madaeni, R. Moradian, S. Zinadini, B. Astinchap, Novel antibifouling
678 nanofiltration polyethersulfone membrane fabricated from embedding TiO2 coated multiwalled
679 carbon nanotubes, Sep. Purif. Technol. 90 (2012) 69-82
680 https://doi.org/10.1016/j.seppur.2012.02.014.

681 [43] N. Sani, W. Lau, A. Ismail, Polyphenylsulfone-based solvent resistant nanofiltration (SRNF)
682 membrane incorporated with copper-1, 3, 5-benzenetricarboxylate (Cu-BTC) nanoparticles for
683 methanol separation, RSC Adv. 5 (2015) 13000-13010 https://doi.org/10.1039/C4RA14284E.

684 [44] F. Zhao, E. Repo, Y. Song, D. Yin, S.B. Hammouda, L. Chen, S. Kalliola, J. Tang, K.C. Tam,
685 M. Sillanpää, Polyethylenimine-cross-linked cellulose nanocrystals for highly efficient recovery
686 of rare earth elements from water and a mechanism study, Green Chem. 19 (2017) 4816-4828
687 https://doi.org/10.1039/C7GC01770G.

688 [45] K.A. Curtis, D. Miller, P. Millard, S. Basu, F. Horkay, P.L. Chandran, Unusual salt and pH
689 induced changes in polyethylenimine solutions, PloS one 11 (2016) e0158147
690 https://doi.org/10.1371/journal.pone.0158147.

691 [46] J. Suh, H.-j. Paik, B.K. HwANG, Ionization of Poly (ethylenimine) and Poly (allylamine) at
692 Various pH′ s, Bioorg. Chem. 22 (1994) 318-327 https://doi.org/10.1006/bioo.1994.1025.

693 [47] S. Zhao, Y. Yao, C. Ba, W. Zheng, J. Economy, P. Wang, Enhancing the performance of
694 polyethylenimine modified nanofiltration membrane by coating a layer of sulfonated poly (ether
695 ether ketone) for removing sulfamerazine, J. Membr. Sci. 492 (2015) 620-629
696 https://doi.org/10.1016/j.memsci.2015.03.017.

697 [48] K.P. Sharma, C.K. Choudhury, S. Srivastava, H. Davis, P. Rajamohanan, S. Roy, G.
698 Kumaraswamy, Assembly of polyethyleneimine in the hexagonal mesophase of nonionic
699 surfactant: effect of pH and temperature, J. Phys. Chem. B 115 (2011) 9059-9069
700 https://doi.org/10.1021/jp202614x.

[49] A. Von Zelewsky, L. Barbosa, C. Schläpfer, Poly (ethylenimines) as Brønsted bases and as ligands for metal ions, Coord. Chem. Rev. 123 (1993) 229-246 https://doi.org/10.1016/0010-8545 (93)85057-B.

[50] W. Li, P. Liu, H. Zou, P. Fan, W. Xu, pH sensitive microporous polypropylene membrane prepared through ozone induced surface grafting, Polym. Adv. Technol. 20 (2009) 251-257 https://doi.org/10.1002/pat.1258.

[51] D. Quintanar-Guerrero, B.N. Zorraquín-Cornejo, A. Ganem-Rondero, E. Piñón-Segundo, M.G. Nava-Arzaluz, J.M. Cornejo-Bravo, Controlled release of model substances from pH-sensitive hydrogels, J. Mex. Chem. Soc. 52 (2008) 272-278.

[52] W. Zou, Y. Huang, J. Luo, J. Liu, C. Zhao, Poly (methyl methacrylate–acrylic acid–vinyl pyrrolidone) terpolymer modified polyethersulfone hollow fiber membrane with pH sensitivity and protein antifouling property, J. Membr. Sci. 358 (2010) 76-84 https://doi.org/10.1016/j.memsci.2010.04.028.

[53] E. Shepherd, J. Kitchener, 474. The ionization of ethyleneimine and polyethyleneimine, J. Chem. Soc. (Resumed) (1956) 2448-2452 https://doi.org/10.1039/JR9560002448.

[54] L. Krasemann, B. Tieke, Selective ion transport across self-assembled alternating multilayers of cationic and anionic polyelectrolytes, Langmuir 16 (2000) 287-290 https://doi.org/10.1021/la991240z.

[55] A. Toutianoush, B. Tieke, Pervaporation separation of alcohol/water mixtures using self-assembled polyelectrolyte multilayer membranes of high charge density, Mater. Sci. Eng. C 22 (2002) 459-463 https://doi.org/10.1016/S0928-4931 (02)00189-3.

722 [56] W.F. Reed, S. Ghosh, G. Medjahdi, J. Francois, Dependence of polyelectrolyte apparent
723 persistence lengths, viscosity, and diffusion on ionic strength and linear charge density,
724 Macromolecules 24 (1991) 6189-6198 https://doi.org/10.1021/ma00023a021.

725 [57] J. Nagaya, M. Homma, A. Tanioka, A. Minakata, Relationship between protonation and ion
726 condensation for branched poly (ethylenimine), Biophys. Chem. 60 (1996) 45-51
727 https://doi.org/10.1016/0301-4622 (95)00143-3.